

Seasonal Observations of carbonate chemistry and ocean acidification in 2012

Prepared for

ConocoPhillips Company
P.O. Box 100360
Anchorage, AK 99510-0360

Shell Exploration & Production Company
3601 C Street, Suite 1334
Anchorage, AK 99503

And

Statoil Alaska
3800 Centerpoint, Suite 920
Anchorage, AK 99503

FINAL REPORT

Prepared by:

Jeremy T. Mathis
Director
Ocean Acidification Research Center
University of Alaska Fairbanks
School of Fisheries and Ocean Sciences
245 O'Neill BLDG
Fairbanks, AK 99775-7220
Phone: (907) 474-5926
jtmathis@alaska.edu

October 2013

EXECUTIVE SUMMARY

Samples were collected and analyzed for dissolved inorganic carbon (DIC) and total alkalinity (TA) in August and September in Burger, Klondike, and Statoil study areas, as well as the expanded study area in the northeastern and southwestern Chukchi Sea. These samples were used to calculate the pH, partial pressure of carbon dioxide ($p\text{CO}_2$), and carbonate mineral saturation states (Ω) for calcite and aragonite in the water column. The data were consistent with recent studies in the region that showed primary production from phytoplankton in late spring significantly alters the carbon biogeochemistry of the water column throughout the year. Early in the ice-free period, primary production consumes DIC in the euphotic zone causing pH and carbonate mineral saturation states to increase. However, much of the organic matter that is produced is exported from the surface making the eastern Chukchi Sea a strong sink for atmospheric CO_2 . As the organic matter settles near the bottom and is broken down by bacteria, DIC concentrations increase sharply, particularly later in the year, driving down pH and suppressing the concentrations of important carbonate minerals that are necessary for shell growth in benthic calcifying organisms. Data from 2012 show a definitive seasonal progression of aragonite becoming undersaturated along the bottom in September. While carbonate saturation states would naturally be suppressed by high rates of export production, penetration of anthropogenic CO_2 into the water column (ocean acidification) has caused the observed undersaturations. These undersaturations will likely expand as CO_2 levels in the atmosphere continue to rise in the coming decades. It is unclear what the implications of ocean acidification will be with respect to benthic calcifying organisms.

TABLE OF CONTENTS

Executive Summary	2
Introduction.....	4
Background.....	5
Methods.....	10
Results.....	13
Discussion.....	16
Concluding Remarks.....	18
References.....	34

INTRODUCTION

The Arctic Ocean plays an important and likely increasing role in both the regional and global climate system with complex and poorly constrained interactions and feedbacks between sea-ice, the ocean and atmosphere, and the hydrological cycle. Some of these interactions have a significant impact on the global balance and atmospheric concentrations of greenhouse gases such as carbon dioxide (CO₂). Currently, the Arctic basin is an important sink for atmospheric CO₂ with recent estimates suggesting that the region contributes between 5 to 14% to the global ocean's net uptake of CO₂ (Bates and Mathis, 2009). In the lease areas being studied as part of the CSESP, the Chukchi Sea appears to be a strong seasonal sink for atmospheric CO₂.

The uptake of CO₂ by the Arctic Ocean is of particular importance because since the Industrial Revolution the oceans have absorbed approximately 127 Petagram (Pg) (Pg = 10¹⁵ g C) of CO₂ from the atmosphere (Sabine and Feely, 2007). While this has mitigated the increase in atmospheric CO₂ concentrations by ~55% (Sabine et al., 2004; Sabine and Feely, 2007), it has changed the carbonate chemistry of seawater chemical speciation (e.g. Caldiera and Wickett, 2003; Andersson and Mackenzie, 2004; Feely et al., 2004; Orr et al., 2005; Millero, 2007) with unknown, but potentially significant impacts to current and future marine ecosystems (Fabry et al., 2008, 2009; Cooley and Doney, 2009). The absorption of atmospheric CO₂ by the ocean has resulted in a lowering of pH, especially over the last few decades (e.g., Bates, 2007; Byrne et al., 2010) as atmospheric CO₂ levels have risen sharply, with a subsequent decrease in the availability of carbonate ions (CO₃²⁻) and a suppression of the saturation states (Ω) of calcium carbonate minerals (CaCO₃), which could result in a reduction of suitable habitat for marine calcifiers. These processes, collectively termed "ocean acidification" (OA), have occurred naturally over geologic time scales (e.g. Zachos et al., 2005) but have been accelerated due to increasing emissions from industrial processes and changes in land use (Feely et al., 2004; Sabine et al. 2004; Orr et al., 2005; Caldiera and Wickett, 2005). Because of these rapid environmental changes, the arctic marine carbon cycle will likely enter a transition period in the coming decades, with large uncertainties in the exchange of atmosphere-ocean CO₂ (Anderson and Kaltin, 2001; Bates et al., 2006; Bates and Mathis, 2009; Cai et al., 2010; Jutterstrom and Anderson, 2010) in response to sea-ice

loss and other climate change induced processes, such as warming temperatures and changes in primary production. Furthermore, the Arctic marine carbon cycle and marine ecosystems are also vulnerable to ocean acidification that results from the uptake of CO₂ from the atmosphere (Orr et al., 2005; Steinacher et al., 2009; Bates et al., 2009; Yamamoto-Kawai et al., 2009).

BACKGROUND

The Arctic Ocean occupies approximately 2.6% of the surface area of the global ocean, but contains <1% of the total ocean volume. It is a Mediterranean type sea that is almost completely surrounded by landmasses, with only few communication points with other ocean basins. Given its geographical layout, it is disproportionately impacted by terrestrial fluxes and receives almost 10% of the total global river runoff annually from an extensive system of rivers and smaller coastal streams that drain the watersheds of eastern Siberia and northwestern North America (McGuire et al., 2006; Cooper et al., 2008). However, these discharges are episodic, with the majority of the total flux occurring in late spring and summer. The landmasses surrounding the Arctic basin contain large stores of terrestrial carbon and strongly influence the biogeochemical dynamics of the marine carbon cycle. For half the year, the Arctic Ocean is almost completely covered by sea-ice with only small areas of open water in the form of polynyas and flaw leads. This seasonal sea-ice cover plays a major role in controlling the carbon cycle through vertical homogenization of the water-column by physical processes such as ventilation, brine rejection and convective mixing. In the western Arctic (i.e. Chukchi Sea), seasonal atmospheric warming and the inflow of warm, lower salinity waters from Pacific sources leave the broad Chukchi shelf nearly sea-ice free for most of the summer months.

The wide and shallow Chukchi Sea occupies a particularly extensive portion of the marginal western Arctic Ocean. Relatively warm and nutrient-rich Pacific Ocean waters enter the Chukchi Sea, flowing northward through Bering Strait from the Bering Sea (Coachman et al., 1975; Roach et al., 1995; Woodgate et al., 2005). As such, the physics and carbon biogeochemistry of the Chukchi Sea are highly influenced by this inflow and can be characterized as an "inflow" shelf (Carmack and Wassmann, 2006;

Bates and Mathis, 2009). Inflow of Pacific Ocean water through Bering Strait into the Chukchi Sea delivers $\sim 0.8\text{-}1.0 \text{ Pg C yr}^{-1}$ of inorganic carbon into the Arctic Ocean (Bates and Mathis, 2009), with outflow from the western Arctic primarily through the Canadian Archipelago. In comparison, rates of primary production from marine phytoplankton and ice algae have been determined to be $\sim 135 \text{ Tg C yr}^{-1}$ ($\text{Tg} = 10^{12} \text{ g}$) in the entire Arctic Ocean, although there are large uncertainties in these estimates (Macdonald *et al.*, 2010). The arctic landmasses contain even larger stores of carbon compared to the marine environment, and there are significant river inputs of organic carbon to the Arctic shelves (e.g., Lobbes *et al.*, 2000; Among, 2004; Rachold *et al.*, 2004; Guo and Macdonald, 2006; Raymond *et al.*, 2007; Holmes *et al.*, 2008). Pan-arctic river inputs of carbon have been estimated by McGuire *et al.* (2009) at 33 Tg C yr^{-1} of DOC and $43.2 \text{ Tg C yr}^{-1}$ DIC, which are 7.1% and 10.6% of their respective total global total river fluxes (Cai *et al.*, 2011). River inputs of particulate organic carbon (POC) and coastal erosion of terrestrial carbon (mostly refractory organic carbon) have also been estimated at $\sim 12 \text{ Tg C yr}^{-1}$ (e.g., Rachold *et al.*, 2004; Macdonald *et al.*, 2010). Arctic rivers thus contribute disproportionately large amounts of carbon to the Arctic Ocean compared to other ocean basins. Compared to many other open-ocean and coastal environments, relatively few studies of the marine carbon cycle have been conducted in the western Arctic. The harsh polar climate and difficult logistical support have limited most studies to opportunistic icebreaker surveys conducted on the Arctic Ocean shelves during the summertime sea-ice retreat. Even with large scale, multiyear projects such as the Shelf-Basin Interactions (SBI II) (Grebmeier *et al.*, 2008), spring and summer observations of the marine carbon cycle in the Arctic Ocean are highly limited and virtually absent during fall and winter. Thus, there are considerable uncertainties about the physical and biological controls on the marine carbon cycle, natural and human perturbed seasonal and interannual variability, CO_2 sinks and sources in the Arctic Ocean and ocean acidification.

Biological Production

The inflow of nutrient-rich water from the Pacific Ocean into the Chukchi Sea (Codispoti *et al.*, 2005), coupled with near constant light in summer supports a brief, but

intensive period of marine phytoplankton photosynthesis and growth compared to other shelves of the Arctic Ocean (Cota et al., 1996; Hill and Cota, 2005) where nutrients are more limited. Occupying the base of the food web, primary production rates of phytoplankton on the Chukchi Sea shelf can exceed $>300 \text{ g C m}^2 \text{ y}^{-1}$ or $0.3\text{-}2.8 \text{ g C m}^2 \text{ d}^{-1}$ (e.g., Hameedi, 1978; Cota et al., 1996; Gosselin et al., 1997; Hill and Cota, 2005; Bates et al., 2005; Mathis et al., 2009; Macdonald et al., 2010). Intense seasonal growth of marine phytoplankton supports a large zooplankton biomass that in turn supports diverse open water and seafloor ecosystems (Feder et al., 2005; Grebmeier et al., 2008). Both pelagic and benthic ecosystems on the Chukchi Sea shelf support marine mammal (e.g., gray whale, walrus, and polar bears), seabird and human populations in the region. In the Chukchi Sea, the brief period of high rates of marine phytoplankton primary production results in the formation of high concentrations of suspended particulate organic carbon (sPOC) (Bates *et al.*, 2005; Moran et al., 2005; Lepore et al., 2007) (Figure 1). High concentrations of sPOC have been observed (up to 2000 mg C L^{-1} ; average of $\sim 200\text{-}300 \text{ mg C L}^{-1}$) across the shelf, with considerable export of sPOC off the shelf into the Canada Basin (Bates et al., 2005b), and relatively high rates of vertical export of organic carbon to shelf, slope and basin sediments (Moran et al., 2005; Lepore et al., 2007). The ecosystem is dominated by large sized phytoplankton (Grebmeier et al., 2008) that produce a relatively large size class of organic matter (i.e., as POC) that is rapidly exported to bottom waters over the shelf.

Pigment analysis of phytoplankton is a well-established technique to map phytoplankton populations and distributions, and to monitor their abundance and composition (Wright, 2005). In the past, these parameters have been determined by microscopy. However, microscopy is time-consuming and some species are too small to be identified via microscopy. Pigments are used as biomarkers of phytoplankton groups and while some pigments are unique markers of one phytoplankton group (such as peridinin for dinoflagellates), most of the pigments are shared between groups (such as fucoxanthin for diatoms and prymnesiophytes) (Jeffrey, 1994). Pigment concentrations, which are used in this study, provide a qualitative abundance of each phytoplankton group.

Air-Sea Fluxes of CO₂

The export character of the shelf conditions the surface waters of the Chukchi Sea to be a strong sink for atmospheric CO₂. Early studies of the Chukchi Sea (Semiletov 1999) showed that seawater $p\text{CO}_2$ (~200-350 μatm) ($\mu\text{atm} = 10^{-6} \text{ atm}$) values were lower than the atmosphere (~365-380 μatm at the time of observation) during the sea-ice free period. Since then, other studies have observed similarly low seawater $p\text{CO}_2$ conditions on the Chukchi Sea shelf during summer (~150-350 μatm ; Pipko et al., 2008; Murata and Takizawa, 2003; Bates et al., 2005a; Bates, 2006; Chen and Gao, 2007; Fransson et al., 2009; Andreev et al., 2010). Large drawdowns of surface water DIC from primary production is the main controller of $p\text{CO}_2$ values in summer (Bates et al., 2005; Bates, 2006; Cai et al., 2010). The seasonal changes in DIC have been largely attributed to high rates of primary production of phytoplankton or net community production (Bates et al., 2005; Mathis et al., 2007), especially in the vicinity of Barrow Canyon (at the northern edge of the Chukchi Sea shelf; Bates et al., 2005; Hill and Cota, 2005), which is close to the lease areas. However, the seasonal decrease in $p\text{CO}_2$ values is somewhat moderated by warming temperatures that drive $p\text{CO}_2$ values higher. The seasonal rebound of seawater $p\text{CO}_2$ and DIC during wintertime likely results from the uptake of CO₂ from the atmosphere and winter mixing induced from brine rejection (Anderson et al., 2004; Omar et al., 2007). Early season observations in the Chukchi Sea indicate that these processes return the surface waters to near saturation compared to atmospheric $p\text{CO}_2$ values before ice retreat and the onset of the spring bloom. After the bloom, summertime $p\text{CO}_2$ values are typically in the range of -50 to -200 μatm relative to the atmosphere, creating a strong driving force for air-sea exchange. Previous estimates of the rates of air-sea CO₂ exchange during the sea-ice free period in the summertime have ranged from approximately -20 to -90 mmol CO₂ m⁻² d⁻¹ (mmol = 10⁻³ mol) (Wang et al., 2003; Murata and Takizawa, 2003; Bates, 2006; Fransson et al., 2009) indicating that the surface waters of the Chukchi Sea shelf have the potential to be a strong sink of atmospheric CO₂ (Kaltin and Anderson, 2005). The annual ocean CO₂ uptake for the Chukchi Sea shelf has been estimated at 2-9 mmol C m⁻² yr⁻¹ (Katlin and Anderson, 2005; Bates, 2006), or approximately 11 to 53 Tg C yr⁻¹. These studies show that the Chukchi Sea shelf dominates air-sea CO₂ fluxes in the western Arctic region.

Ocean Acidification

The drawdown of DIC during the spring phytoplankton bloom has a significant impact on water column pH and the saturation states of the two most important carbonate minerals (calcite and aragonite). As DIC is consumed, $p\text{CO}_2$ drops in the surface layer causing pH to increase, raising the saturation states of calcite and aragonite. In response to high export production, the remineralization of organic matter increases the concentration of DIC and $p\text{CO}_2$ in bottom waters and suppresses carbonate mineral saturation states to a varying degree across the Chukchi shelf. In the region near the head of Barrow Canyon, export production is highest and this is where the strongest seasonal suppression of aragonite in subsurface water has been observed. This suppression of carbonate mineral saturation states corresponds to high apparent oxygen utilization (AOU) rates and elevated silicate in the bottom waters indicating both pelagic and benthic remineralization. The subsurface effects of remineralization can be especially significant during periods of intense production when saturation states increase at the surface. These biologically driven, seasonally divergent trajectories of Ω , or the “Phytoplankton-Carbonate Saturation State” (PhyCaSS) Interaction, have been observed in the Chukchi Sea (Bates *et al.*, 2009; Bates and Mathis, 2009), and are likely typical of highly productive polar and sub-polar shelves. The PhyCaSS Interaction could be particularly influential on benthic calcifiers in the Chukchi Sea because the lowest saturation states coincide with areas of highest export production. It appears that the export production, which provides the food source at the bottom, is causing the undersaturation that could inhibit shell and test growth in calcifying organisms.

This PhyCaSS Interaction is now being exacerbated by the penetration of CO_2 into the oceans, particularly in high latitude regions. The decrease in seawater pH due to the uptake of CO_2 (Bindoff *et al.*, 2007; Bates, 2007) has been termed “ocean acidification” and has been observed at several open ocean time-series locations (e.g. Bermuda Atlantic Time Series (BATS) and the Hawaii Ocean Time Series (HOTS)). The uptake of CO_2 has already decreased surface water pH by 0.1 units when averaged across the global ocean. Intergovernmental Panel on Climate Change (IPCC) scenarios, based on present-day CO_2 emissions, predict a further decrease in seawater pH by 0.3 to 0.5 units over the next century and beyond (Caldeira and Wickett, 2003). Ocean acidification

and decreased pH reduces the saturation states of calcium carbonate minerals such as aragonite and calcite, with many studies showing decreased CaCO_3 production by calcifying fauna (Buddemeier et al., 2004; Fabry et al., 2008) and increased CaCO_3 dissolution. The Arctic Ocean is particularly vulnerable to ocean acidification due to relatively low pH and low temperature of polar waters compared to other waters (Orr et al., 2005; Steinacher et al., 2009) and low buffer capacity of sea-ice melt waters (Yamamoto-Kawai et al., 2009).

In the Arctic Ocean, potentially corrosive waters are found in the subsurface layer of the central basin (Jutterstrom and Anderson, 2010; Yamamoto-Kawai et al., 2009; Chierici and Fransson, 2009), on the Chukchi Sea shelf (Bates et al., 2009) and in outflow waters of the Arctic found on the Canadian Arctic Archipelago shelf (Azetsu-Scott et al., 2010). On the Chukchi Sea, waters corrosive to CaCO_3 occur seasonally in the bottom waters with unknown impacts to benthic organisms. As described above, the seasonally high rates of summertime phytoplankton primary production in the Chukchi Sea drives a downward export of organic carbon, which is remineralized back to CO_2 which in turn increases seawater $p\text{CO}_2$ (and decreasing pH) of subsurface waters. Such a seasonal biological influence on the pH of subsurface waters amplifies existing impacts of ocean acidification induced by the uptake of CO_2 over the last century (Bates et al., 2009). Given the scenarios for pH changes in the Arctic, the Arctic Ocean and adjacent arctic shelves including the western Arctic, will be increasingly affected by ocean acidification, with potentially negative implications for shelled benthic organisms as well as those animals that rely on the shelf seafloor ecosystem.

METHODS

Cruise Information and Water Column Sampling

Physical, chemical and biological measurements were made during cruises (1202, 1203, and 1204) to the study area in August and September of 2012 (Figure 2). Samples for DIC and TA were collected at all three studies sites in August and only at the expanded study sites in September. Seawater samples for DIC/TA were drawn from Niskin bottles into pre-cleaned ~300 mL borosilicate bottles. These samples were subsequently poisoned with mercuric chloride (HgCl_2) to halt biological activity, sealed,

and returned to the laboratory for analysis. All sampling and analysis was performed in compliance with the guide to best practices for ocean acidification research and reporting (Riebesell et al., 2010). Pigment (phytoplankton) samples were collected by filtering three liters of seawater through 47mm glass fiber filters. The filters were stored in liquid nitrogen.

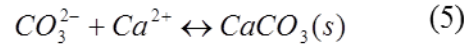
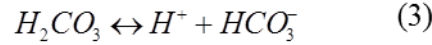
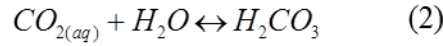
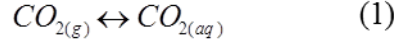
Laboratory Analysis and Calculation of Carbonate Parameters

DIC and TA samples were analyzed using a precise and accurate gas extraction/coulometric detection system (Bates, 2001). The analytical system consists of a VINDTA 3C (Versatile Instrument for the Detection of Total Alkalinity; <http://www.marianda.com>) coupled to a CO₂ coulometer (model 5012; UIC Coulometrics). TA samples were also determined by potentiometric titration using the VINDTA 3C. Routine analyses of Certified Reference Materials (CRMs, provided by A.G. Dickson, Scripps Institution of Oceanography) ensured that the accuracy of the DIC and TA measurements were within 0.05% ($\sim 1 \mu\text{mol kg}^{-1}$, $\mu\text{mol} = 10^{-6} \text{ mol}$) and stable over time. Seawater $p\text{CO}_2$, pH and CaCO₃ saturation states for calcite (Ω_{calcite}) and aragonite ($\Omega_{\text{aragonite}}$) were calculated from DIC, TA, temperature, salinity, phosphate, and silicate data using the thermodynamic model of Lewis and Wallace (1995). The carbonic acid dissociation constants of Mehrbach *et al.* (1973) [refit by Dickson and Millero, 1987; i.e., pK1 and pK2] were used to determine the carbonate parameters. The CO₂ solubility equations of Weiss (1974), and dissociation constants for borate (Dickson, 1990), silicate and phosphate (Dickson and Goyet, 1994) were used as part of the calculations. Uncertainty in the calculation of Ω_{calcite} and $\Omega_{\text{aragonite}}$ were ~ 0.02 .

Pigment samples were analyzed using High Performance Liquid Chromatography (HPLC). The filters were extracted into acetone for 16 hours in a -20 °C freezer. The samples were filtered and 1000 μL were mixed with 300 μL of milliQ water and 200 μL of the mixed solution were injected into the Agilent HPLC instrument. Pigment concentrations were calculated from peak areas obtained from the phytoplankton pigment standards.

Basis of the Arctic Marine Carbonate System

As CO₂ levels rise in the atmosphere, the increased pCO₂ in seawater contributes to OA and the suppression of biologically important carbonate mineral concentrations, such as calcite and aragonite, through a series of well-known reactions:



Following dissolution (Eq. 1), dissolved CO₂ undergoes hydration reactions to form carbonic acid (Eq. 2), which rapidly dissociates to form carbonate and releases hydrogen ions (Eqs. 3, 4). Almost all of the produced carbonate ions react with calcium to form mineral solids (Eq. 5), preventing this reaction from contributing to dissolved alkalinity. Further, most of the free hydrogen ions produced react with the naturally dissolved alkalinity in seawater, reducing carbonate ion concentrations. The remaining hydrogen ions contribute to the lowering of pH. Carbonate mineral saturation states are dependent on the concentration of free carbonate ions according to the following equations, such that a reduction in available CO₃²⁻ (Eq. 5) decreases the saturation states of both aragonite and calcite:

$$\Omega_{aragonite} = \frac{[Ca^{2+}][CO_3^{2-}]}{K^*_{SP_{aragonite}}} \quad (6)$$

$$\Omega_{calcite} = \frac{[Ca^{2+}][CO_3^{2-}]}{K^*_{SP_{calcite}}} \quad (7)$$

Cold ocean temperatures increase the solubility of CO₂ and precondition the seawater to have lower calcium carbonate concentrations and saturation states compared to more temperate ocean environments, leaving polar and sub-polar shelves particularly vulnerable to OA (Orr *et al.*, 2005; Bates and Mathis, 2009; Fabry *et al.*, 2009; Steinacher *et al.*, 2009). In addition to this temperature effect, several other processes affect the

carbonate system and can contribute to the intensification of OA in polar and sub-polar regions, including seasonally high rates of primary production, river runoff, and sea-ice formation and melt processes (e.g. Bates and Mathis, 2009; Bates et al., 2009). For example, seasonally intense periods of primary production are uncoupled from grazing in most polar environments (e.g., Springer *et al.*, 1996; Macdonald *et al.*, 2010) leading to high rates of organic matter export from the surface layer (e.g. Mathis et al., 2007). While this export production supports the biologically diverse benthic communities in these regions it leads to elevated rates of remineralization in bottom waters and sediments. Thus, ocean biology tends to drive seasonally divergent trajectories for seawater chemistry, with primary production in the euphotic zone increasing Ω in the mixed layer while an accumulation of DIC in subsurface waters through remineralization suppresses Ω (e.g. Bates et al., 2009). The reduction and undersaturation of carbonate minerals, particularly in bottom waters of polar and sub-polar seas could have implications for benthic ecosystems. Further decreases in pH and Ω could have significant consequences for the benthic and pelagic ecosystems in a region where organisms are already struggling to adapt to changing environmental conditions (Løvorn *et al.*, 2003; Moore *et al.*, 2003; Overland and Stabeno, 2004; Grebmeier *et al.*, 2006).

RESULTS

August cruise (Cruise 1202)

Bottom DIC and TA gradually increased in concentration from the southernmost stations of Klondike to the northernmost stations of Burger and Statoil, while bottom pH and Ω_{arag} decreased (Figure 3). The lowest bottom DIC and TA concentrations were found at Klondike ($\text{DIC}^{\text{min}} = 2003 \mu\text{moles kg}^{-1}$; $\text{TA}^{\text{min}} = 2217 \mu\text{moles kg}^{-1}$). The average bottom DIC and TA were higher at Statoil ($\text{DIC}^{\text{mean}} = 2226 \mu\text{moles kg}^{-1}$; $\text{TA}^{\text{mean}} = 2287 \mu\text{moles kg}^{-1}$) than at Burger ($\text{DIC}^{\text{mean}} = 2189 \mu\text{moles kg}^{-1}$; $\text{TA}^{\text{mean}} = 2275 \mu\text{moles kg}^{-1}$), while maximum concentrations of DIC and TA were found at Burger, reaching $2298 \mu\text{moles kg}^{-1}$ and $2318 \mu\text{moles kg}^{-1}$, respectively. Salinity was also highest at Burger ($S^{\text{max}} = 33.37$), with a small decrease towards the south at Klondike ($S^{\text{min}} = 32.28$). Temperature was negatively correlated with DIC, TA and salinity and progressively decreased from south Klondike to north Statoil ($T^{\text{max}} = 4.6^{\circ}\text{C}$, $T^{\text{min}} = -1.7^{\circ}\text{C}$) (Figure 4).

This pattern was accompanied by highest $p\text{CO}_2$, and lowest pH and Ω_{arag} values at Burger ($p\text{CO}_2^{\text{max}} = 920 \mu\text{atm}$; $\text{pH}^{\text{min}} = 7.68$; $\Omega_{\text{arag}}^{\text{min}} = 0.58$). Bottom waters undersaturated with respect to aragonite were found at Burger and Statoil, while Ω_{arag} remained oversaturated in Klondike, ranging between 1.73 and 2.35. Bottom waters at Burger were also undersaturated with regard to calcite ($\Omega_{\text{calc}}^{\text{min}} = 0.93$) and were very close to calcite undersaturation ($\Omega_{\text{calc}}^{\text{min}} = 1.01$) at Statoil.

At the surface, the carbonate chemistry followed an opposite pattern than was observed at the bottom (Figure 5). The highest values of DIC and TA were found at Klondike, with a maximum of $1992 \mu\text{moles kg}^{-1}$ and $2118 \mu\text{moles kg}^{-1}$, respectively. At Statoil, surface DIC and TA concentrations were lowest ($\text{DIC}^{\text{min}} = 1734 \mu\text{moles kg}^{-1}$; $\text{TA}^{\text{min}} = 1951 \mu\text{moles kg}^{-1}$). Temperature was also lowest at Statoil and highest at Klondike, ranging from -0.18°C to 6.6°C (Figure 6). A $p\text{CO}_2$ minimum value of $86.6 \mu\text{atm}$ was observed at Statoil, while the maximum value of $266.9 \mu\text{atm}$ was measured at Burger. pH and Ω_{arag} increased from Klondike to Statoil. All surface waters were supersaturated with regard to aragonite, with lowest levels of 1.71 found at Burger. The highest chlorophyll-*a* concentrations were found north of Burger and Statoil ($\text{chl } a^{\text{max}} = 376.2 \text{ ng L}^{-1}$), which was accompanied by high fucoxanthin and alloxanthin concentrations ($\text{fux}^{\text{max}} = 98.7 \text{ ng L}^{-1}$; $\text{alx}^{\text{max}} = 16.4 \text{ ng L}^{-1}$), suggesting the presence of diatoms and cryptophytes (Figure 11).

September cruises (Cruises 1203 and 1204)

September bottom observation showed a similar pattern as in August with an increase of DIC and TA concentrations from south to north while pH and Ω_{arag} decreased. The highest bottom DIC and TA concentrations, $2302 \mu\text{moles kg}^{-1}$ and $2299 \mu\text{moles kg}^{-1}$ respectively, were found in the northern part of Hanna Shoal, along with the lowest temperatures ranging between -1.7 and -1.2°C (Figures 7 and 8). TA concentrations in Herald Shoal and the central area showed little variability, ranging between 2250 and $2260 \mu\text{moles kg}^{-1}$ respectively, whereas DIC values were more variable, ranging between 2106 and $2156 \mu\text{moles kg}^{-1}$. This pattern was followed by the highest $p\text{CO}_2$ levels ($p\text{CO}_2^{\text{max}} = 1157.8 \mu\text{atm}$), highest salinities ($S^{\text{max}} = 33.31$) and lowest pH and Ω_{arag} ($\text{pH}^{\text{min}} = 7.58$; $\Omega_{\text{arag}}^{\text{min}} = 0.47$) in Hanna Shoal. Bottom waters undersaturated with regard to

aragonite were found in Hanna Shoal, while Ω_{arag} remained supersaturated in Herald Shoal, ranging from 1.17 to 2.10. Waters remained oversaturated with regard to calcite, except in Hanna Shoal, where Ω_{calc} reached a minimum of 0.75.

At the surface, the DIC and TA followed an opposite pattern than was observed at the bottom (Figure 9). The lowest surface DIC and TA concentrations were found in Hanna Shoal, with a minimum of 1736 $\mu\text{moles kg}^{-1}$ and 1882 $\mu\text{moles kg}^{-1}$ respectively, accompanied by the lowest temperatures and salinities with minima of 0.2°C and 26.77 respectively (Figure 10). The highest concentrations of TA and DIC were found in Herald Shoal, where surface water is warm and salty ($\text{DIC}^{\text{max}} = 2011 \mu\text{moles kg}^{-1}$; $\text{TA}^{\text{max}} = 2211 \mu\text{moles kg}^{-1}$; $T^{\text{max}} = 5.4^\circ\text{C}$; $S^{\text{max}} = 32.04$). Surface pH averaged 8.25 in the whole study area, and ranged between $\text{pH}^{\text{min}} = 8.18$, close to the coast, and $\text{pH}^{\text{max}} = 8.66$, in north Hanna Shoal. The lowest pH and Ω_{arag} values were found in Hanna Shoal ($\text{pH}^{\text{min}} = 8.18$; $\Omega_{\text{arag}}^{\text{min}} = 1.37$). All surface waters were supersaturated with regard to aragonite, with a maximum of 2.37 found in Herald Shoal area. The high Ω_{arag} were accompanied by high chlorophyll a concentrations ($\text{chl}^{\text{a max}} = 2039 \text{ ng.L}^{-1}$), with highest concentrations of fucoxanthin and 19'-hexfucoxanthin ($\text{fux}^{\text{max}} = 806 \text{ ng.L}^{-1}$; $19\text{hex}^{\text{max}} = 238 \text{ ng.L}^{-1}$), which correspond to high abundance of diatoms and prymnesiophytes respectively (Figure 12).

Depth profiles showed a gradual increase of $p\text{CO}_2$, DIC and TA in both months, while pH and Ω_{arag} decrease (Figures 13-17). In August, TA and DIC reached maximum concentrations below 30 m depth ($\text{DIC}^{\text{max}} = 2348 \mu\text{moles kg}^{-1}$; $\text{TA}^{\text{max}} = 2318 \mu\text{moles kg}^{-1}$). At the surface, TA ranged between 1887 and 2210 $\mu\text{moles kg}^{-1}$, whereas TA only varied between 2210 and 2308 $\mu\text{moles kg}^{-1}$ along the seafloor. $p\text{CO}_2$ showed an opposite pattern and ranged between and 124.0 and 924.1 μatm near the bottom.

September observations along the DBO line showed that surface DIC concentrations increased slightly from Wainwright to Burger, with a minimum concentration of 1821 $\mu\text{moles kg}^{-1}$ close to the coast to a maximum of 2028 $\mu\text{mol.kg}^{-1}$ offshore, while the highest TA, $p\text{CO}_2$ and salinities were found close to Wainwright ($\text{TA}^{\text{max}} = 2142 \mu\text{moles kg}$; $p\text{CO}_2 = 262.4 \mu\text{atm}$; $S^{\text{max}} = 31.8$) (Figure 9). This pattern was followed by a decrease of temperature with a maximum of 4.2°C close to shore and a minimum of 0.4 off shore (Figure 10). This pattern was accompanied by the lowest pH values found near-shore ($\text{pH}^{\text{min}} = 8.18$). The aragonite saturation state was similar

through the water column close to the coast and at the surface to Burger ($\Omega_{\text{arag}} = 2$). Undersaturated waters with respect to aragonite were found further off shore below 30m depth with Ω_{arag} decreasing gradually and reaching a minimum at Burger ($\Omega_{\text{arag}}^{\text{min}} = 0.70$). After 30m depth, DIC and TA reach the highest values 2266 and 2287 $\mu\text{moles kg}^{-1}$ respectively, corresponding to a lower pH ($\text{pH}^{\text{min}} = 7.8$) and water close to undersaturation (Figure 16). Salinity and temperature showed the same feature with cold water after 30 m ($T^{\text{min}} = -1.4^{\circ}\text{C}$) and higher salinity ($S^{\text{max}} = 33.07$) (Figure 18).

DISCUSSION

The combination of several biological and physical drivers, such as production and remineralization of organic matter, changes in temperature, intrusion of different water masses, sea ice melt and riverine input all induced the large observed variability in the carbonate parameters. High biological productivity along the sea ice margin counteracted the effect of sea ice melt water, resulting in relatively high pH and Ω_{arag} at the northern most stations in both August and September (Figures 5 and 6). The low salinity, temperature and TA levels at the northern sites suggest that a significant amount of sea ice melt water was present. These sites also showed a high chlorophyll-*a* concentration, mostly due to high abundances of diatoms and cryptophytes right at the sea ice edge. High productivity decreased DIC and counteracted the TA-reducing sea ice melt effect, resulting in higher pH and carbonate mineral saturation states at these ice affected locations.

The combination of respiration of organic matter, water depth and some upwelling of deep Canada Basin water strongly influenced the northern part of the Chukchi Shelf with CO_2 -rich water, leading to undersaturation with regard to aragonite (Figure 18). High salinity, DIC and TA concentrations were well correlated with the cold-water signal observed along the seafloor in the Hanna Shoal region and along the DBO line. The overall increase of bottom DIC and pCO_2 between August and September is most likely due to remineralization of organic material at depth. However, additional oxygen measurements, or any other sort of data describing remineralization processes, would need to be taken in order to confirm this hypothesis.

A comparison of the last two field seasons suggests that in 2012, conditions in the northern Chukchi Sea were characterized by a strong sea-ice melt signal, enhancing stratification; whereas in 2011, waters were well mixed. Stronger physical processes, such as increased wind mixing and seasonal storm events, had a greater impact on the water column of the Chukchi shelf in 2011. Surface values for $p\text{CO}_2$ in 2011 were higher than in 2012, most likely due to mixing of remineralized CO_2 from the bottom to the surface. These findings highlight the dynamic nature of this marine ecosystem, especially on an interannual timescale.

Timing of Ice Retreat

As a strong low salinity and cold water signal in the surface waters from ice melt was present in 2012, the timing of sea-ice retreat has a substantial effect on carbonate chemistry in subsurface waters. Ice retreat exerts a significant control on the fate of the organic matter produced during the phytoplankton blooms. Zooplankton grazing on seasonal production is minimal during blooms associated with colder surface water temperatures. This is favorable for the benthic ecosystem. In contrast, warmer years increase zooplankton production by up to 50%. Thus, colder waters are expected to be associated with higher export production to the benthos, and large remineralization signals will be generated at depth, corresponding to increases in $p\text{CO}_2$ and decreases in carbonate mineral saturation states. Warmer water blooms will retain carbon in the mixed layer and contribute to increased pelagic production and reduced bottom water remineralization. Variation in the timing of sea-ice retreat could change the mode of production over the shelf. The earlier retreat of sea ice in recent years indicates that the blooms have been occurring in colder water, favoring export of production. If ice continues to retreat earlier in the spring, it could lead to a dichotomy for benthic organisms. On the one hand, higher rates of export production should lead to increased food supply and an expansion of biomass. However, if high rates of export production coupled to increasing CO_2 inventories over the shelf cause expanded aragonite undersaturations it could lead to a reduction in habitat.

CONCLUDING REMARKS

The carbonate datasets collected during the 2010, 2011 and 2012 surveys of the lease sites in the Chukchi Sea show the dynamic nature of the carbon cycle of the western Arctic Ocean. Brief, but intense, periods of primary production in the surface layer in late spring sets the stage for most of the processes that occur during the subsequent ice-free period. The consumption of DIC derived from phytoplankton dramatically lower the $p\text{CO}_2$ of the surface waters promoting broad regions of air-sea exchange and making the Chukchi Sea a strong sink for atmospheric CO_2 . The removal of DIC also raises the pH and carbonate mineral saturation states, counteracting the effects of ocean acidification in the surface waters. However, the disconnects between primary production of phytoplankton and zooplankton grazing cause large quantities of organic matter to be exported from the mixed layer to the seafloor. When this organic matter is remineralized by bacteria, it adds DIC back to the water column, lowering pH and suppressing carbonate mineral saturation states near the bottom.

The Chukchi Sea has been productive for thousands of years and the remineralization of organic matter and the seasonal suppression of carbonate mineral saturation states are natural phenomena. However, the rising inventory of CO_2 in the water column has begun to drive saturation states past a threshold that will likely be detrimental to some marine calcifiers, particularly the diverse benthic organisms that dominate the Chukchi Sea fauna. While ocean acidification is a global issue, the Arctic Ocean will likely experience the physical manifestations and potential impacts of it much sooner than more temperate regions and may be a bellwether of how the global ocean will respond.

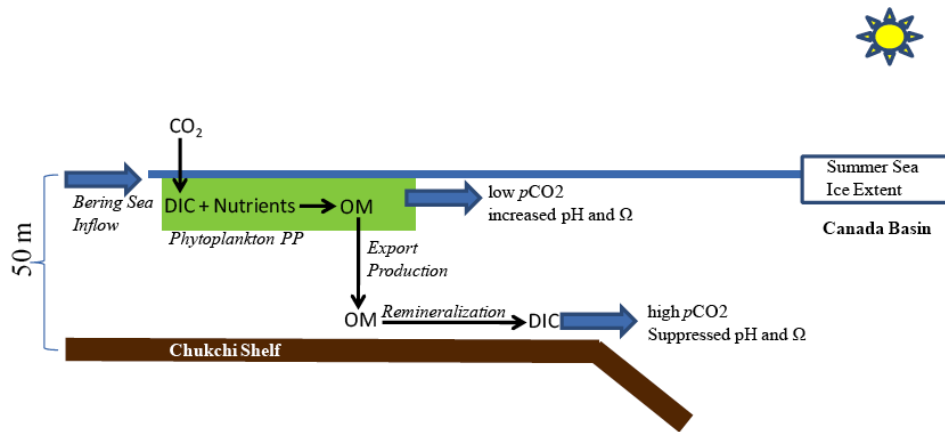


Figure 1. Schematic of the influences on the carbon cycle in the Chukchi Sea. High rates of primary production (green box) consumes DIC, lowering the $p\text{CO}_2$ of the surface waters and promoting air-sea exchange. However, air-sea exchange happens much slower than primary production leaving the surface waters undersaturated with respect to atmospheric CO_2 for most of the summer. The removal of DIC from the surface water causes pH and carbonate mineral saturation states to increase. Due to limited grazing in the water column, most of the organic matter produced by the phytoplankton is exported to depth where it is remineralized back into DIC, increasing the $p\text{CO}_2$ of the bottom waters while lowering pH and suppressing carbonate mineral saturation states. Both the surface and bottom water masses are exported off of the Chukchi shelf conditioning the surface waters under the ice in the deep Canada Basin to be undersaturated with respect to atmospheric CO_2 and the upper halocline of the western Arctic Ocean to be undersaturated in aragonite.

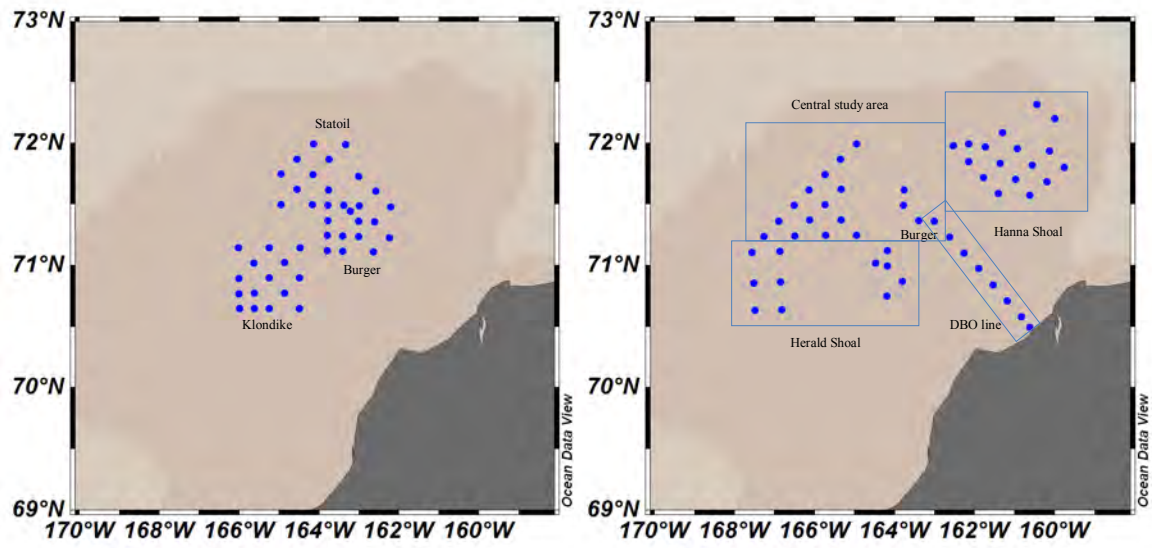


Figure 2. Location of the study areas where carbon measurements were taken in 2012 (Cruises 1202, 1203, and 1204).

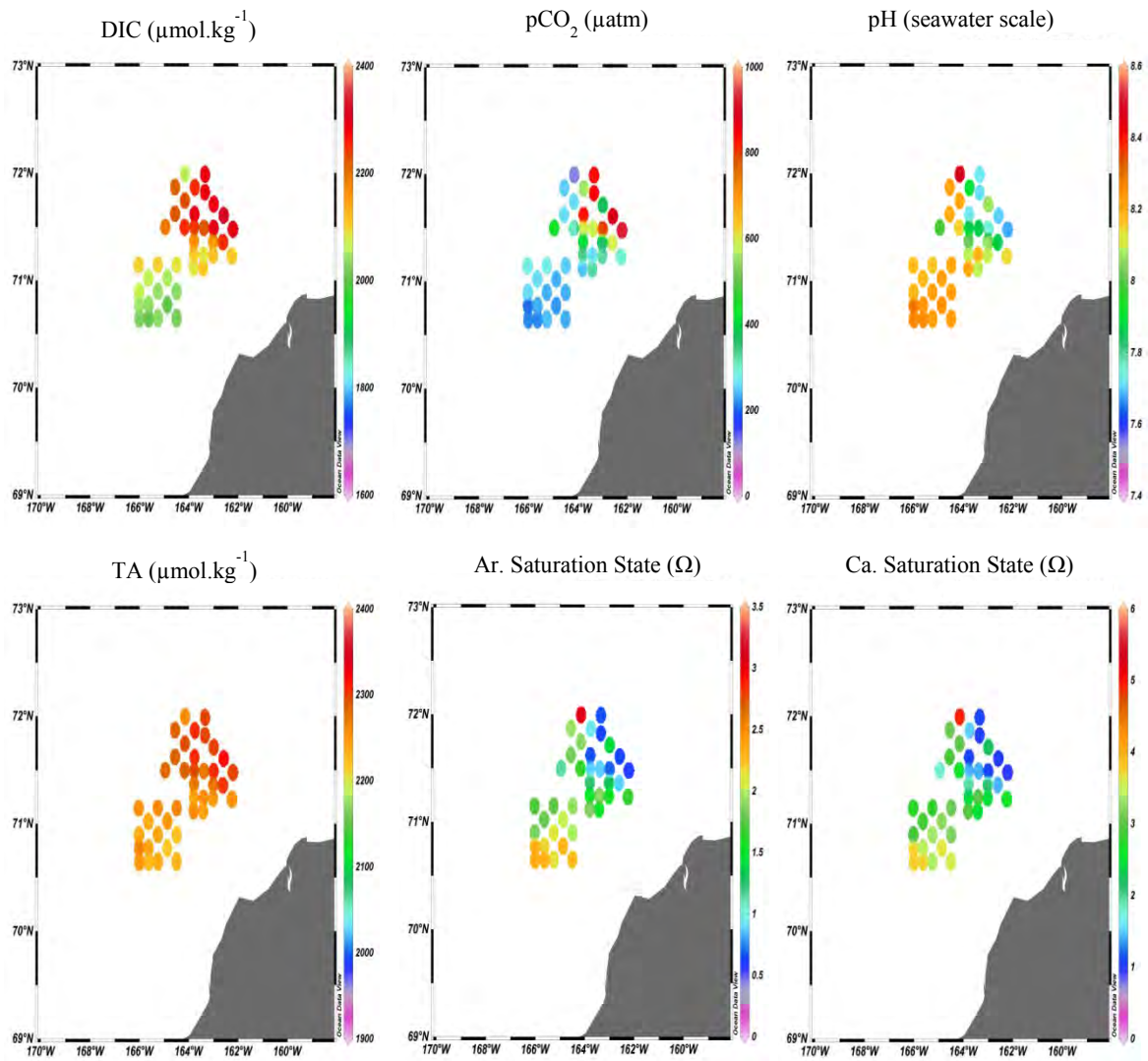


Figure 3. Observations of DIC and TA ($\mu\text{mol.kg}^{-1}$) and calculated values for $p\text{CO}_2$ (μatm), pH (seawater scale), calcite saturation state (Ω), and aragonite saturation state (Ω) along the bottom in August (cruise 1202).

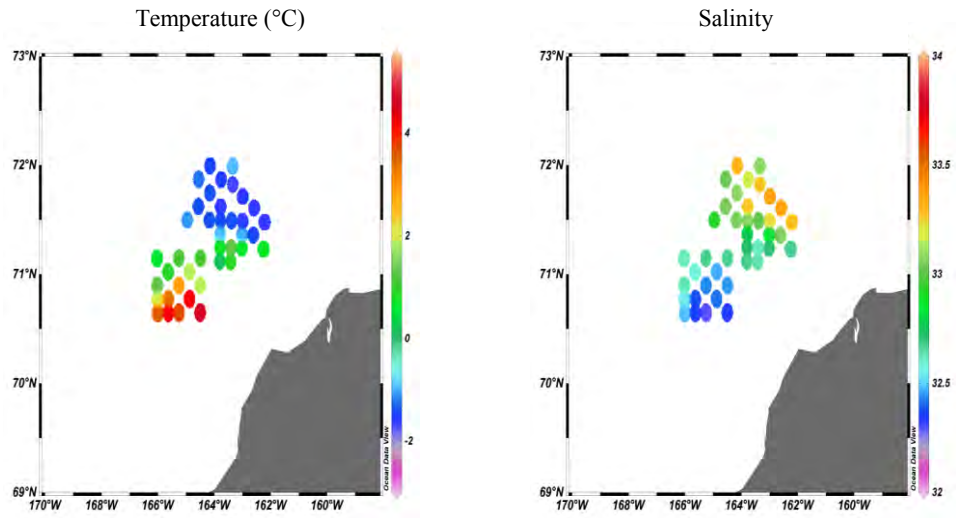


Figure 4. Observations of temperature (°C) and salinity along the bottom in August.

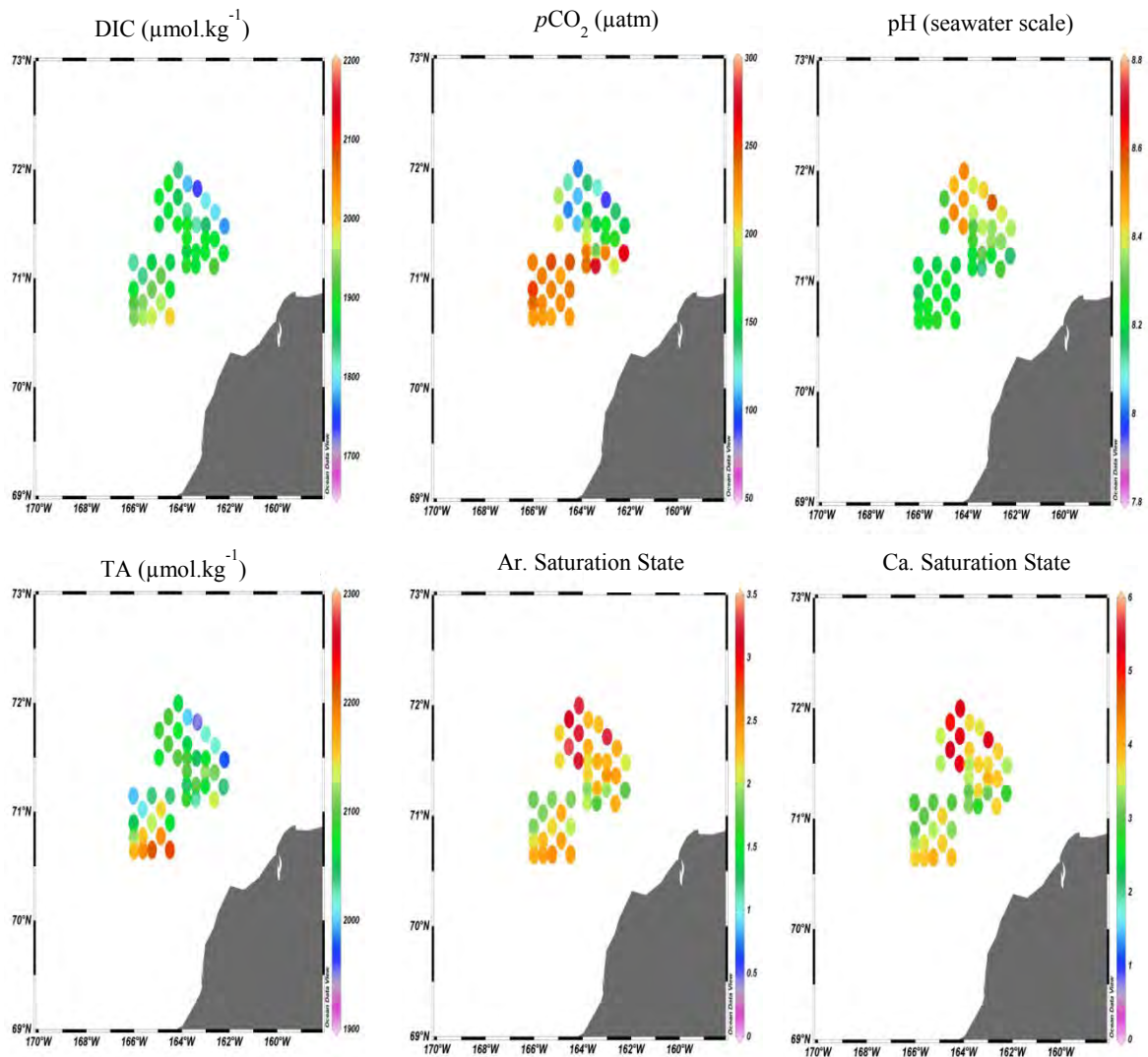


Figure 5. Observations of DIC and TA ($\mu\text{mol.kg}^{-1}$) and calculated values for $p\text{CO}_2$ (μatm), pH (seawater scale), calcite saturation state (Ω), and aragonite saturation state (Ω) at the surface in August.

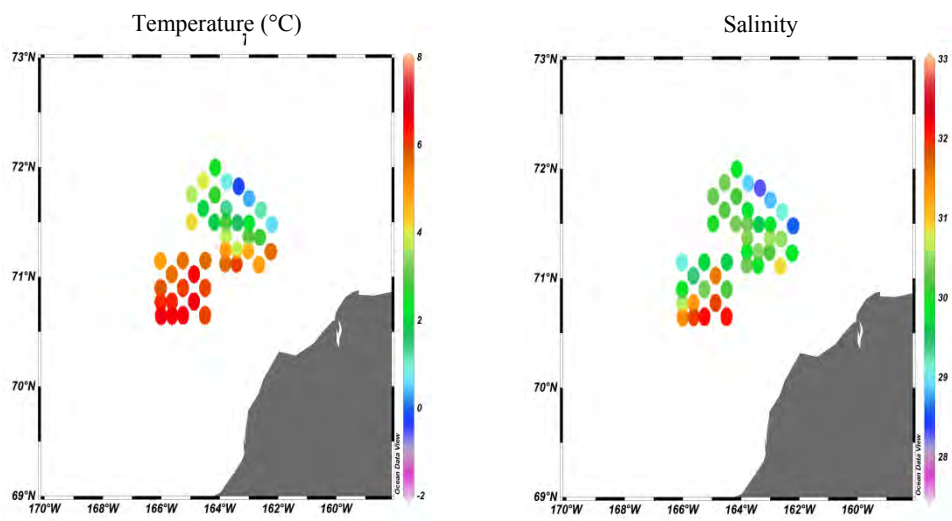


Figure 6. Observations of temperature (°C) and salinity along the surface in August.

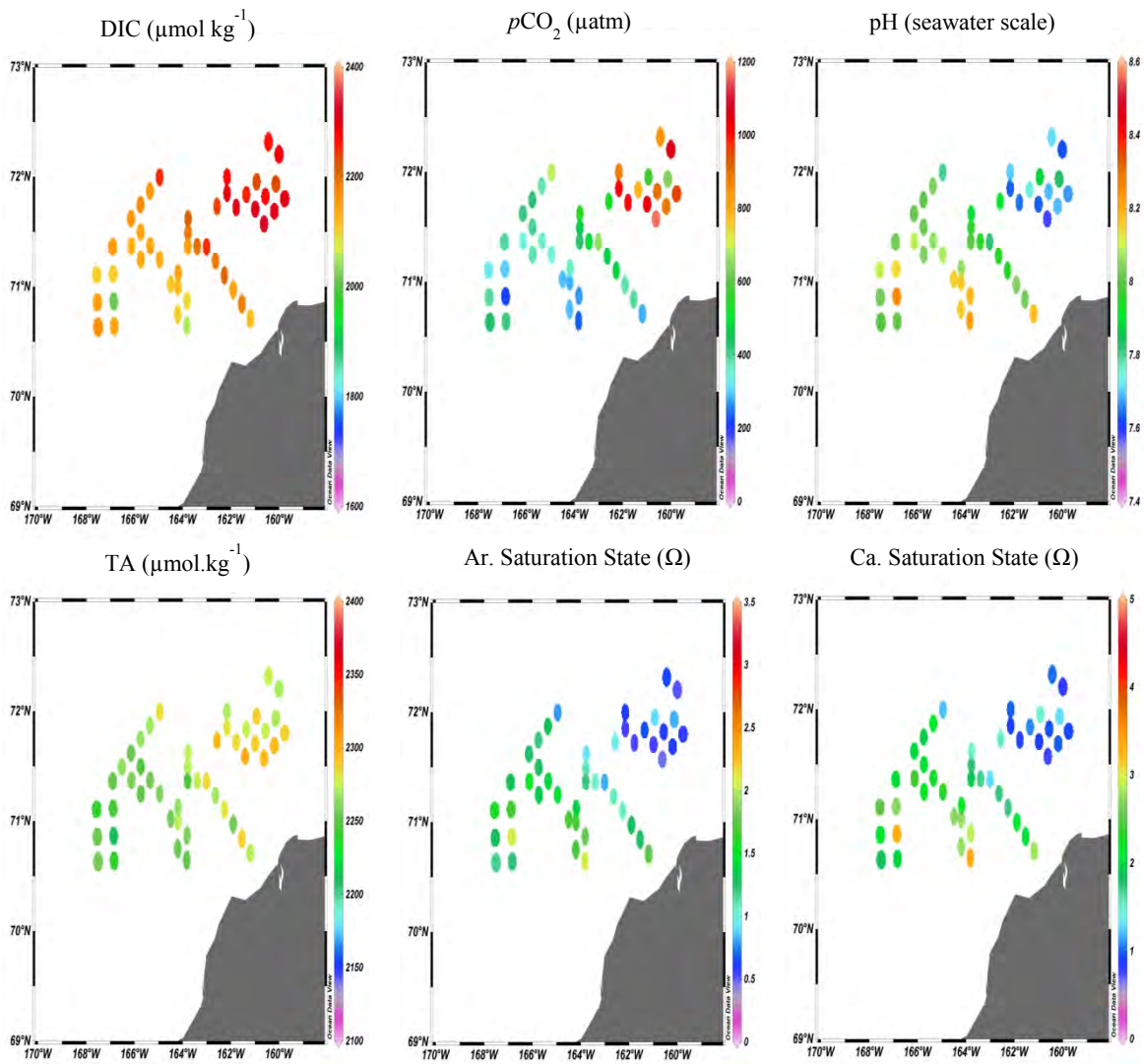


Figure 7. Observations of DIC and TA ($\mu\text{mol kg}^{-1}$) and calculated values for $p\text{CO}_2$ (μatm), pH (seawater scale), calcite saturation state (Ω), and aragonite saturation state (Ω) along the bottom in September.

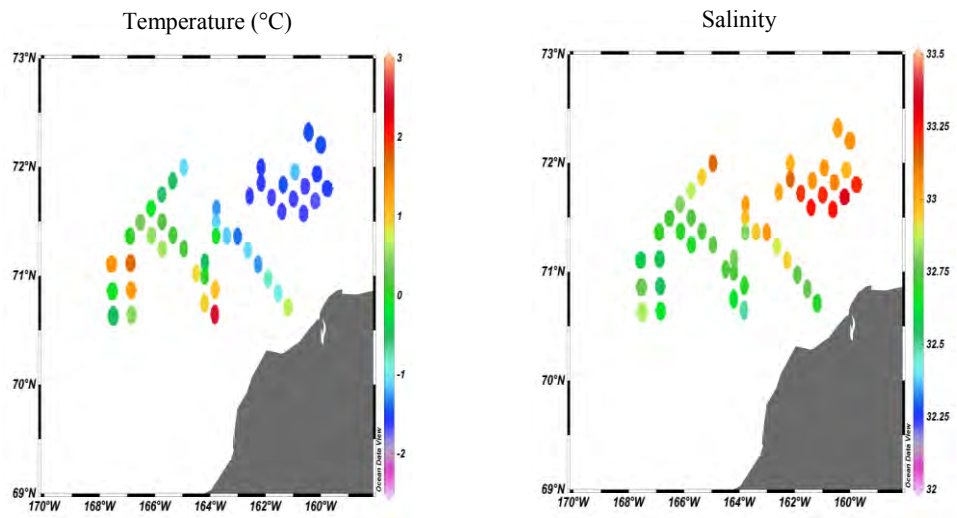


Figure 8. Observations of temperature (°C) and salinity along the bottom in September.

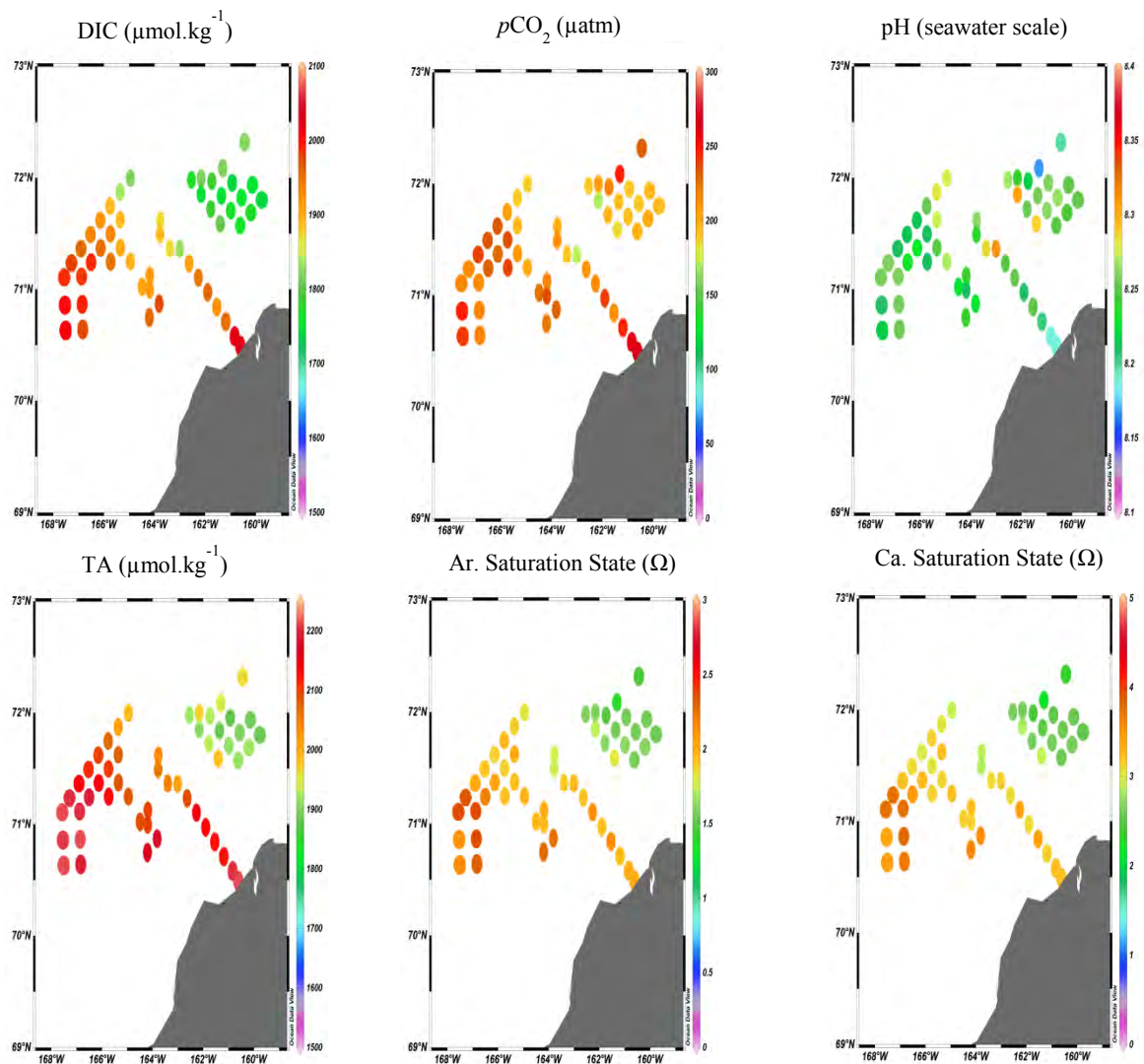


Figure 9. Observations of DIC and TA ($\mu\text{mol.kg}^{-1}$) and calculated values for $p\text{CO}_2$ (μatm), pH (seawater scale), calcite saturation state (Ω), and aragonite saturation state (Ω) along the surface in September (cruises 1203 and 1204).

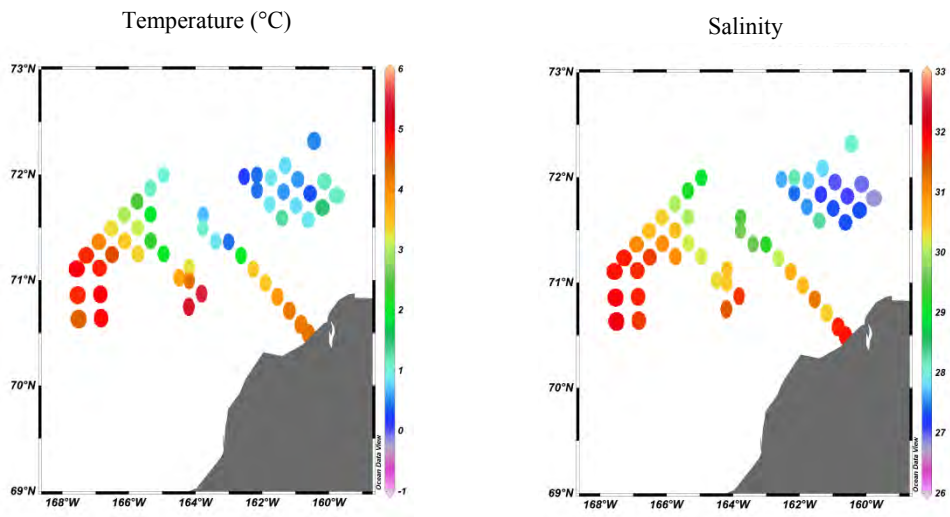


Figure 10. Observations of temperature (°C) and salinity along the surface in September.

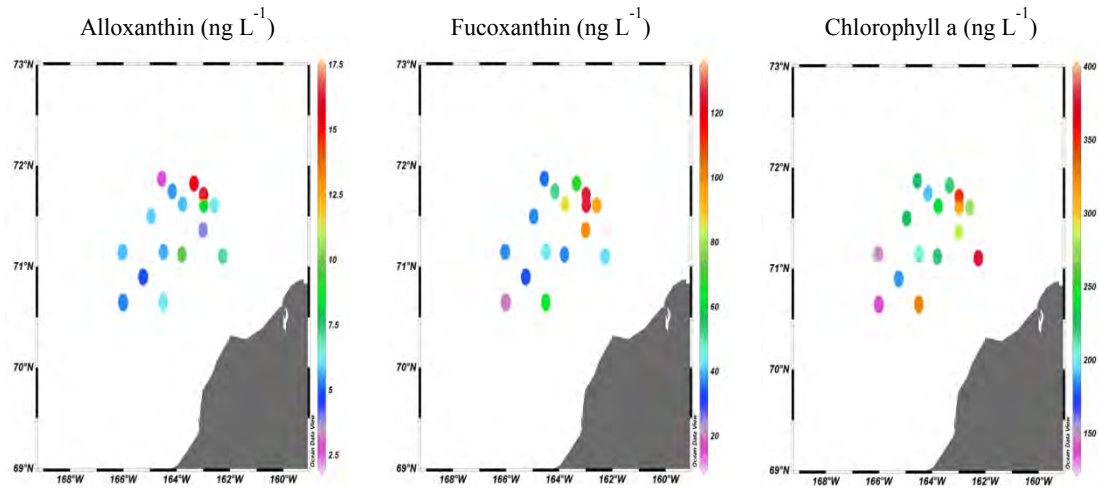


Figure 11. Observations of alloxanthin, fucoxanthin, and chlorophyll a concentrations (ng L⁻¹) along the surface in August (cruise 1202).

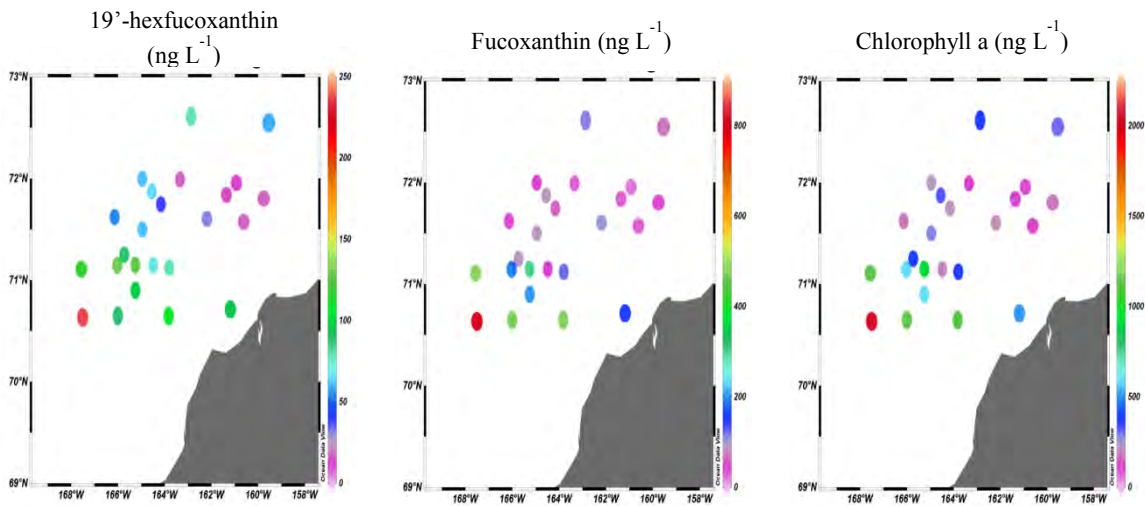


Figure 12. Observations of (a) 19'-hexfucoxanthin, fucoxanthin, and chlorophyll a concentrations (ng L⁻¹) along the surface in September (cruises 1203 and 1204).

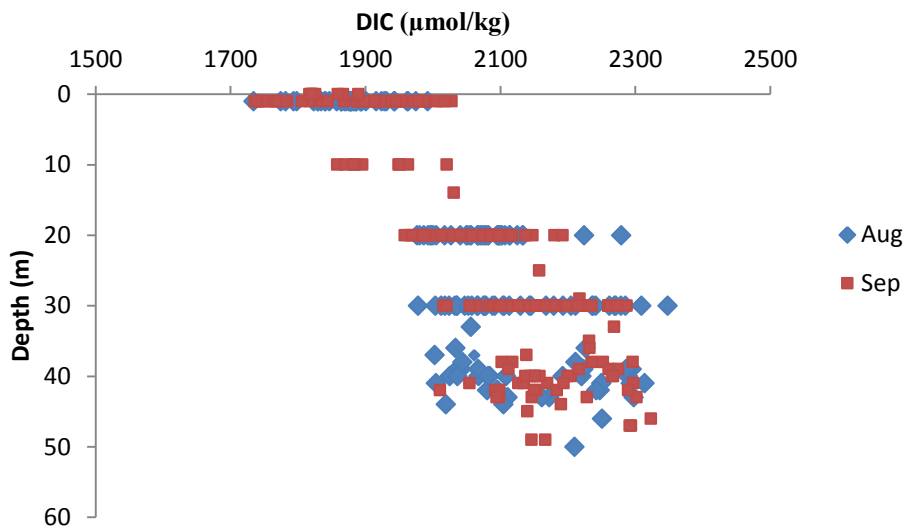


Figure 13. Observed DIC ($\mu\text{mol.kg}^{-1}$) vs. depth (m) in August and September in the study area.

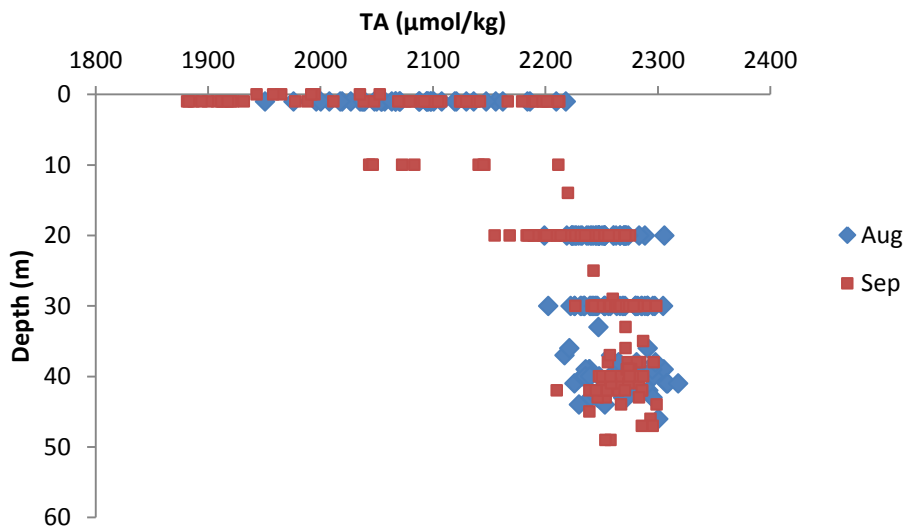


Figure 14. Observed TA ($\mu\text{mol kg}^{-1}$) vs. depth (m) in August and September in the study area.

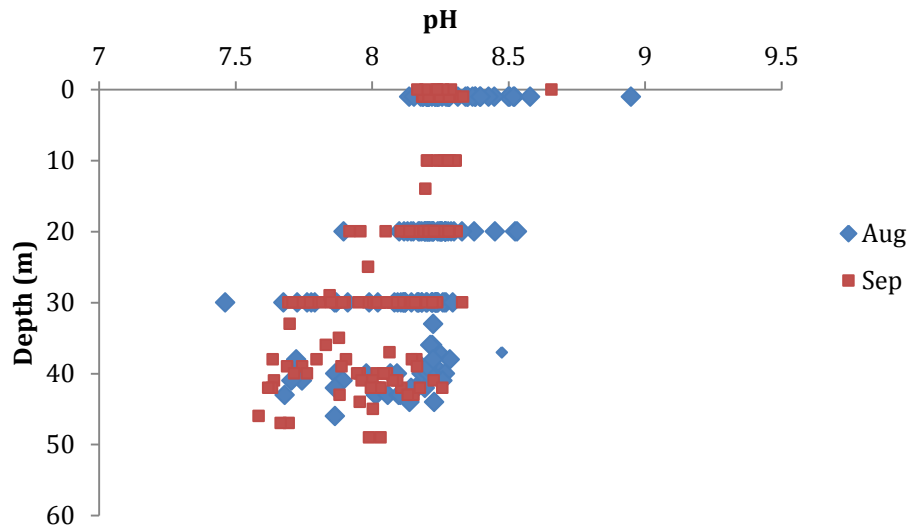


Figure 15. Calculated pH (seawater scale) vs. depth (m) in August and September in the study area.

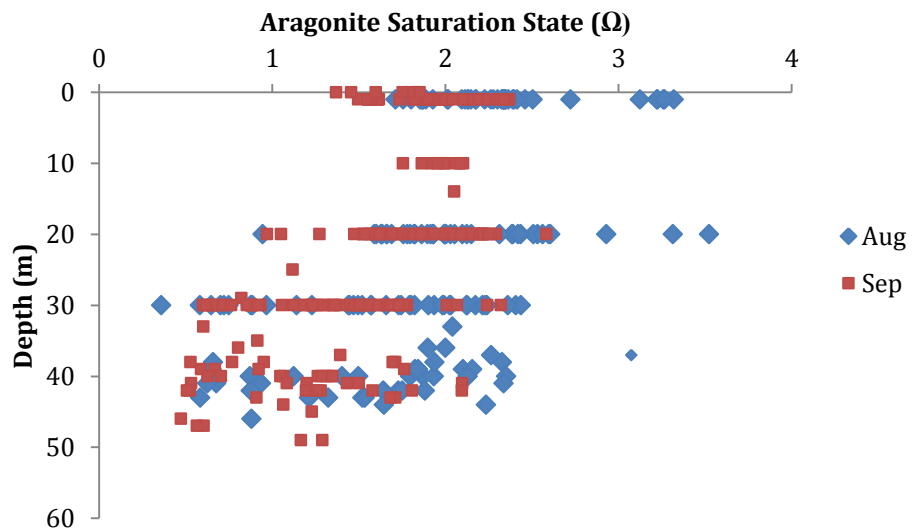


Figure 16. Calculated aragonite saturation state (Ω) vs. depth (m) in August and September in the study area.

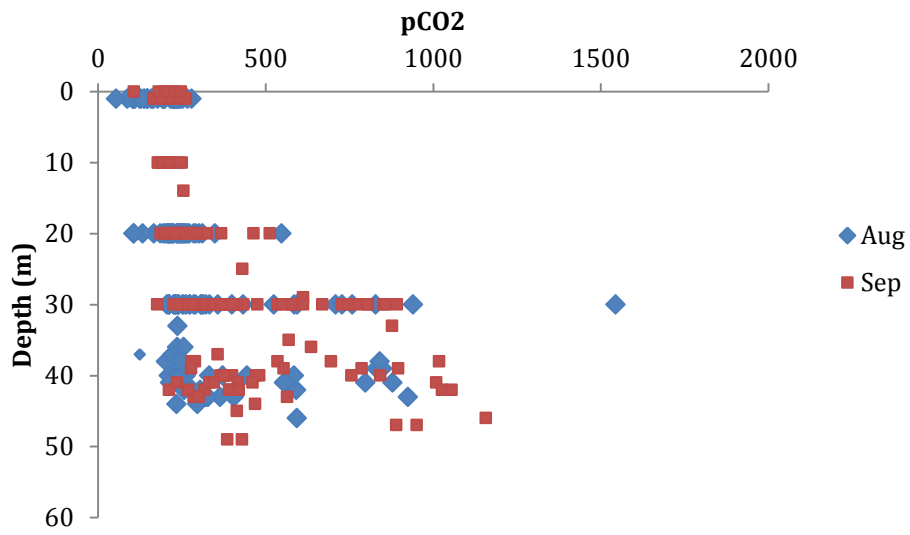


Figure 17. Calculated $p\text{CO}_2$ (μatm) vs. depth (m) in August and September in the study area.

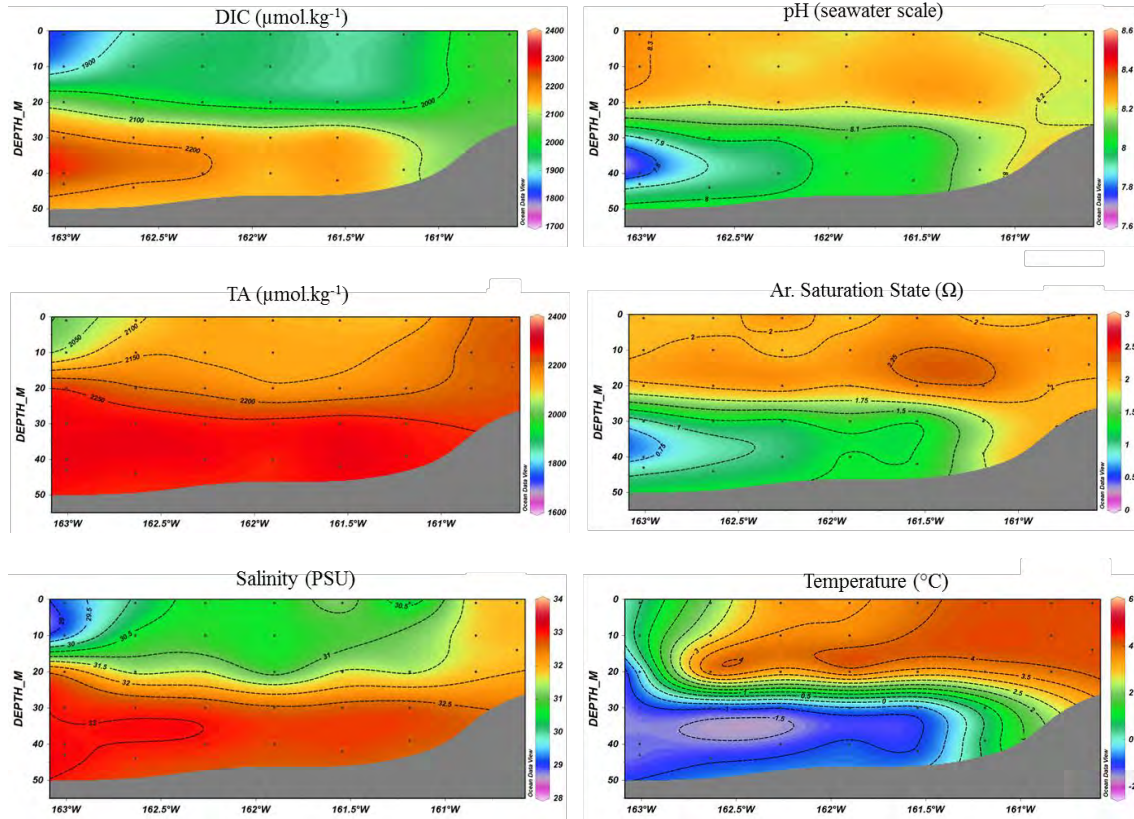
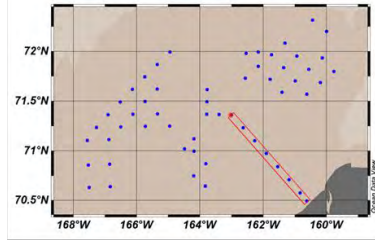


Figure 18. Observations of DIC and TA ($\mu\text{mol.kg}^{-1}$) along with salinity and temperature ($^{\circ}\text{C}$) with calculated values for pH (seawater scale) and aragonite saturation state (Ω) in a section of the DBO line in September.

REFERENCES

- Among, R.M.W., 2004. The role of dissolved organic matter for the organic carbon cycle in the Arctic Ocean, in *The Organic Carbon Cycle in the Arctic Ocean*, edited by R.S. Stein and R.W. Macdonald, pp. 83–99, Springer, New York.
- Anderson, L.G., and Kaitin, S., 2001. Carbon fluxes in the Arctic Ocean - potential impact by climate change. *Polar Research*, **20**(2), 225-232.
- Andersson, A.J., and Mackenzie, F.T., 2004. Shallow-water oceans : a source or sink for atmospheric CO₂? *Frontiers in Ecology and the Environment*, **2**(7), 348–353.
- Andreev, A.G., Chen, C.-T.A., and Sereda, N.A., 2010. The distribution of the carbonate parameters in the waters of Anadyr Bay of the Bering Sea and in the western part of the Chukchi Sea. *Oceanology*, **50**(1), 39-50.
- Azetsu-Scott, K., Clarke, A., Falkner, K., Hamilton, J., Jones, E.P., Lee, C., Petrie, B., Prinsenberg, S., Starr, M., and, Yeats, P. , 2010. Calcium carbonate saturation states in the waters of the Canadian Arctic Archipelago and the Labrador Sea. *Journal of Geophysical Research-Oceans*, **115**, C11021, doi:10.1029/2009JC005917.
- Bates, N.R., 2001. Interannual variability of oceanic CO₂ and biogeochemical properties in the Western North Atlantic subtropical gyre. *Deep-Sea Research II*, **48**, 1507–1528.
- Bates, N.R., Best, M.H.P., and Hansell, D.A., 2005. Spatio-temporal distribution of dissolved inorganic carbon and net community production in the Chukchi and Beaufort Seas. *Deep-Sea Research II*, **52**(22-24), 3303-3323, doi:10.1016/j.dsr2.2005.10.005.
- Bates, N.R., Best, M.H.P., and Hansell, D.A., 2006. Suspended Particulate Organic Matter (sPOM) data from Shelf-Basin Interactions (SBI) survey cruises in the Chukchi and Beaufort Seas during 2004. http://www.eol.ucar.edu/projects/sbi/all_data.shtml.
- Bates, N.R., 2006. Air-sea carbon dioxide fluxes and the continental shelf pump of carbon in the Chukchi Sea adjacent to the Arctic Ocean. *Journal of Geophysical Research (Oceans)*, **111**, C10013, doi 10.129/2005JC003083, 12 Oct. 2006.
- Bates, N.R., 2007. Interannual variability of the oceanic CO₂ sink in the subtropical gyre of the North Atlantic Ocean over the last two decades. *Journal of Geophysical Research (Oceans)*, **112** (C9), C09013, doi:2006JC003759, May 4, 2007.
- Bates, N.R., and Mathis, J.T., 2009. The Arctic Ocean marine carbon cycle: Evaluation of air-sea carbon dioxide exchanges, ocean acidification impacts and potential feedbacks. *Biogeosciences*, **6**(11), 2433-2459.
- Bates, N.R., Mathis, J.T., and Cooper, L., 2009. The effect of ocean acidification on biologically induced seasonality of carbonate mineral saturation states in the Western Arctic Ocean. *Journal of Geophysical Research (Oceans)*, **114**, C11007, doi: 10.1029/2008JC004862.
- Bindoff, N.L., Willebrand, J., Artale, V., Cazenave, A., Gregory, J., Gulev, S., Hanawa, K., Le Quéré, C., Levitus, S., Nojiri, Y., Shum, C.K., Talley, L.D., and Unnikrishnan, A., 2007. Observations: Oceanic Climate Change and Sea Level. In: *Climate Change 2007: The Physical Science Basis. Contribution of Working Group I to the Fourth Assessment Report of the Intergovernmental Panel on*

- Climate Change* [Solomon, S., D. Qin, M. Manning, Z. Chen, M. Marquis, K.B. Averyt, M. Tignor and H.L. Miller (eds.)]. Cambridge University Press, Cambridge, United Kingdom and New York, NY, USA.
- Buddemeier, R.W., Kleypas, J.A., and Aronson, R.B., 2004. *Coral Reefs and Global Climate Change: Potential Contributions of Climate Change to Stresses on Coral Reef Ecosystems*, p. 44, (download report at http://www.pewclimate.org/global-warming/indepth/all_reports/coral_reefs/index.cfm). Pew Center on Climate Change.
- Byrne, R.H., Mecking, S., Feely, R.A., and Liu, Z., 2010. Direct observations of basin-wide acidification of the North Pacific Ocean. *Geophysical Research Letters*, **37**, L02601, doi:10.1029/2009GL040999.
- Cai, W.-J., Chen, L., Chen, B., Gao, Z., Lee, S.H., Chen, J., Pierrot, D., Sullivan, K., Wang, Y., Hu, X., Huang, W.-J., Zhang, Y., Xu, S., Murata, A., Grebmeier, J.M., Jones, E.P., and Zhang, H., 2010. Decrease in the CO₂ uptake capacity in an ice-free Arctic Ocean basin. *Science*, **329**, 556, doi: 10.1126/science.1189338.
- Cai, W.-J. 2011. Estuarine and coastal ocean carbon paradox: CO₂ sinks or sites of terrestrial carbon incineration? *Annual Reviews of Marine Science*, **3**, 123-45, doi:10.1146/annurev-marine-120709-142723.
- Caldiera, K. and Wickett, M.E., 2003. Anthropogenic carbon and ocean pH. *Nature*, **425**(6956), 365.
- Caldiera, K., and Wickett, M.E., 2005. Ocean model predictions of chemistry changes from carbon dioxide emissions to the atmosphere and ocean. *Journal of Geophysical Research – Oceans*, **110**(C9), C09S04, doi:10.1029/2004JC002671.
- Carmack, E. and Wassman, P., 2006. Food webs and physical-biological coupling on pan-Arctic shelves: Unifying concepts and comprehensive perspectives. *Progress in Oceanography*, **71**, 446-477. doi:10.1016/j.pocean.2006.10.004.
- Chen, L.Q. and Gao, Z.Y., 2007. Spatial variability in the partial pressures of CO₂ in the northern Bering and Chukchi seas. *Deep-Sea Research II*, **54**(23-26), 2619-2629, doi:10.1016/j.dsr2.2007.08.010.
- Chierici, M., and Fransson, A., 2009. Calcium carbonate saturation in the surface water of the Arctic Ocean: undersaturation in freshwater influenced shelves. *Biogeosciences*, **6**, 2421-2432.
- Coachman, L.K., Aagaard, K., and Tripp, R.B., 1975, *Bering Strait: The Regional Physical Oceanography*, University of Washington Press, Seattle, 169 pp.
- Codispoti, L., Flagg, C., and Kelly, V., 2005. Hydrographic conditions during the 2002 SBI process experiments. *Deep-Sea Research II*, **52** (22-24), 3199-3226.
- Cooley, S.R., and Doney, S.C., 2009. Anticipating ocean acidification's economic consequences for commercial fisheries. *Environmental Research Letters*, **4**, 024007, doi:10.1088/1748-9326/4/2/024007.
- Cooper, L.W., McClelland, J.W., Holmes, R.M., Raymond, P.A., Gibson, J.J., Guay, C.K., and Peterson, B.J., 2008. Flow-weighted values of runoff tracers (d¹⁸O, DOC, Ba, alkalinity) from the six largest Arctic rivers. *Geophysical Research Letters*, **35**, L18606, doi:10.1029/2008GL035007.
- Cota, G.F., Pomeroy, L.R., Harrison, W.G., Jones, E.P., Peters, F., Sheldon W.M., and

- Weingartner T.R., 1996. Nutrients, primary production and microbial heterotrophy in the southeastern Chukchi Sea: Arctic summer nutrient depletion and heterotrophy. *Marine Ecology Progress Series*, **135** (1-3): 247-258.
- Dickson, A.G., and Millero, F.J., 1987. A comparison of the equilibrium constants for the dissociation of carbonic acid in seawater media. *Deep Sea Research Part A*, **34**(10), 1733–1743.
- Dickson, A.G., 1990. Standard potential of the reaction $\text{AgCl(s)} + .5\text{H}_2(\text{g}) = \text{Ag(s)} + \text{HCl(aq)}$ and the standard acidity constant of the ion HSO_4^- in synthetic sea water from 273.15 to 318.15 K: *The Journal of Chemical Thermodynamics*, **22**(2), 113-127.
- Dickson, A.G., and Goyet, C., Eds., 1994. Handbook of Methods for the Analysis of Various Parameters of the Carbon Dioxide System in Seawater, version 2.0. *Rep. ORNL/CDIAC-74*, U.S. Department Of Energy, Washington, D.C.
- Fabry, V.J., Seibel, B.A., Feely, R.A., and Orr, J.C., 2008. Impacts of ocean acidification on marine fauna and ecosystem processes. *ICES Journal of Marine Science*, **65**, 414–432.
- Fabry, V.J., McClintock, J.B., Mathis, J.T., and Grebmeier, J.M., 2009. Ocean Acidification at high latitudes: the Bellwether. *Oceanography*, **22**(4), 160–171.
- Feder, H.M., Jewett S.C., and Blanchard A., 2005. Southeastern Chukchi Sea (Alaska) epibenthos. *Polar Biology*, **28**(5), 402-421.
- Feely, R.A., Sabine, C.L., Lee, K., Berelson, W., Keypas, J., Fabry, V.J., and Millero, F.J., 2004. Impact of anthropogenic CO_2 on the CaCO_3 system in the oceans. *Science*, **305**(5682), 362–266.
- Fransson, A., Chierici, M., and Nojiri, Y., 2009. New insights into the spatial variability of the surface water carbon dioxide in varying sea ice conditions in the Arctic Ocean. *Continental Shelf Research*, **29**(10), 1317-1328
doi:10.1016/j.csr.2009.03.008.
- Gosselin, M., Levasseur, M., Wheeler, P.A., Horner, R.A., and Booth, B.C., 1997. New measurements of phytoplankton and ice algal production in the Arctic Ocean. *Deep-Sea Research II*, **44**, 1623-1644, doi:10.1016/S0967-0645(97)00054-4.
- Grebmeier, J.M., Overland, J.E., Moore, S.E., Farley, E.V., Carmack, E.C., Cooper, L.W., Frey, K.E., Helle, J.H., McLaughlin, F.A., and McNutt, S.L., 2006. A major ecosystem shift in the Northern Bering Sea. *Science*, **311**(5766), 1461–1464.
- Grebmeier, J.M., Bates, N.R., and Devol, A., 2008. Continental Margins of the Arctic Ocean and Bering Sea. In *North American Continental Margins: A Synthesis and Planning Workshop*. U.S. Carbon Cycle Science Program, Washington D.C., (Editors, B. Hales, W.-J. Cai., B.G. Mitchell, C.L. Sabine and O. Schofield, 120 pp), p. 61-72.
- Guo, L., and Macdonald, R.W., 2006. Source and transport of terrigenous organic matter in the upper Yukon River: Evidence from isotope ($\delta^{13}\text{C}$, $\Delta^{14}\text{C}$, and $\delta^{15}\text{N}$) composition of dissolved, colloidal, and particulate phases. *Global Biogeochemical Cycles*, **20**(2), GB2011, doi: 10.1029/2005GB002593.
- Hameedi, M.J., 1978. Aspects of water column primary productivity in Chukchi Sea during summer. *Marine Biology*, **48**(10), 37-46.

- Hill, V., and Cota, G., 2005. Spatial patterns of primary production on the shelf, slope and basin of the Western Arctic in 2002. *Deep-Sea Research II*, **52**(22-24), 3344-3354, doi:10.1016/j.dsr2.2005.10.001.
- Holmes, R.M., McClelland, J.W., Raymond, P.A., Frazer, B.B., Peterson, B.J., and Stieglitz, M., 2008. Lability of DOC transported by Alaskan rivers to the Arctic Ocean. *Geophysical Research Letters*, **35**(3), doi: 10.1029/2007GL032837.
- Jeffrey S. W., Wright S. W. (1994) Photosynthetic pigments in the Haptophyta. In: Green JC, Leadbeater BSC (eds) *The Haptophyte Algae*. Clarendon Press, Oxford, pp 111.
- Jutterstrom, S., and Anderson, L.G., 2010. Uptake of CO₂ by the Arctic Ocean in a changing climate. *Marine Chemistry*, **122** (1-4), 96-104.
- Kaltin, S., and L. G. Anderson, 2005. Uptake of atmospheric carbon dioxide in Arctic shelf seas: Evaluation of the relative importance of processes that influence pCO₂ in water transported over the Bering-Chukchi Sea shelf, *Mar. Chem.*, **94**, 67– 79.
- Lepore, K., Moran, S.B., Grebmeier, J.M., Cooper, L.W., Lalande, C., Maslowski, W., Hill, V., Bates, N.R., Hansell, D.A., Mathis, J.T., and Kelly, R.P., 2007. Seasonal and interannual changes in particulate organic carbon export and deposition in the Chukchi Sea. *Journal of Geophysical Research*, **112**, C10024, doi:10.1029/2006JC003555.
- Lewis, E.R., and Wallace, D.W.R., 1995. Basic programs for the CO₂ system in seawater. Brookhaven National Laboratory, BNL-61827.
- Lobbes, J.M., Fitznar, H.P., and G. Kattner, G., 2000. Biogeochemical characteristics of dissolved and particulate organic matter in Russian rivers entering the Arctic Ocean. *Geochim. Cosmochim. Acta*, **64**(17), 2973-2983.
- Løvvorn, J R., Richman, S.E., Grebmeier, J.M., and Cooper, L.W., 2003. Diet and body condition of Spectacled Eiders wintering in pack ice of the Bering Sea. *Polar Biology*, **26**, 259–267.
- Mathis, J.T., Pickart, R.S., Hansell, D.A., Kadko, D., Bates, N.R., 2007a. Eddy transport of organic carbon and nutrients from the Chukchi Shelf: Impact on the upper halocline of the western Arctic Ocean. *Journal of Geophysical Research*, **112**, C05011, doi: 10.1029/2006JC003899.
- Mathis, J.T., Hansell, D.A., and Bates, N.R., 2009. Interannual variability of dissolved inorganic carbon distribution and net community production during the Western Arctic Shelf-Basin Interactions Project. *Deep-Sea Research II*, **56**(17), 1213-1222, doi:10.1016/j.dsr2.2008.10.017.
- Macdonald, R.W. Anderson, L.G., Christensen, J.P., Miller, L.A., Semiletov, I.P., and Stein, R., 2009. Polar Margins: The Arctic Ocean. In *Carbon and Nutrient Fluxes in Continental Margins: A Global Synthesis*. Liu, K.K., Atkinson, L., Quinones, R., and Talue-McManus, L., (editors), Springer, New York, 291-303.
- McGuire, A.D., Chapin, F.S., Walsh, J.E., and Wirth, C., 2006. Integrated regional changes in arctic climate feedbacks: implications for the global climate system. *Annual Rev. Environmental Resources*, **31**, 61-91.
- McGuire, A.D., Anderson, L., Christensen, T.R., Dallimore, S., Guo, L.D., Hayes, D., Heimann, M., Macdonald, R. and Roulet, N. 2009. Sensitivity of the carbon cycle in the Arctic to climate change (Review). *Ecological Monographs*, **79**(4), 523-555.

- Mehrbach, C., Culberson, C.H., Hawley, J.E., and Pytkowicz, R.M., 1973. Measurement of the apparent dissociation constants of carbonic acid in seawater at atmospheric pressure. *Limnology and Oceanography*, **18**, 897–907.
- Millero, F. J., 2007. The Marine Inorganic Carbon Cycle. *Chemical Reviews*, **107**(2), 308–341.
- Moore, E.E., Gremeier, J.M., and Davis, J.R., 2003. Gray whale distribution relative to forage habitat in the northern Bering Sea: Current conditions and retrospective summary. *Canadian Journal of Zoology*, **81**, 734–742.
- Moran, S.B., Kelly, R.P., Hagstrom, K., Smith, J.N., Grebmeier, J.M., Cooper, L.W., Cota, G.F., Walsh, J.J., Bates, N.R., Hansell, D.A., Maslowski, W., Nelson, R.P., and Mulsow, S., 2005. Seasonal changes in POC export flux in the Chukchi Sea and implications for water column-benthic coupling in Arctic shelves. *Deep-Sea Research*, **52** (22-24), 3427-3451, doi:10.1016/j.dsr2.2005.09.011.
- Murata, A., and Takizawa, T., 2003. Summertime carbon dioxide sinks in shelf and slope waters of the western Arctic Ocean. *Continental Shelf Research*, **23**(8), 753-776.
- Omar, A.M., Johannessen, T., Olsen, A., Kaltin, S., and Rey, F., 2007. Seasonal and interannual variability of the air-sea carbon dioxide flux in the Atlantic sector of the Barents Sea. *Marine Chemistry*, **104**, 203–213, doi:10.1016/j.marchem.2006.11.002.
- Orr, J.C., Fabry, V.J., Aumont, O., Bopp, L., Doney, S.C., Feely, R.A., Gnanadesikan, A., Gruber, N., Ishida, A., Joos, F., Key, R.M., Lindsay, K., Maier-Reimer, E., Matear, R., Monfray, P., Mouchet, A., Najjar, R.G., Plattner, G.K., Rodgers, K. B., Sabine, C.L., Sarmiento, J.L., Schlitzer, R., Slater, R.D., Totterdell, I J., Weirig, M.F., Yamanaka, Y., and Yool, A., 2005. Anthropogenic ocean acidification over the twenty-first century and its impact on calcifying organisms. *Nature*, **437**(7059), 681–686.
- Overland, J.E., and Stabeno, P.J., 2004. Is the climate of the Bering Sea warming and affecting the ecosystem? *Eos, Transactions of the American Geophysical Union*, **85**(33), 309, doi:10.1029/2004EO330001.
- Pipko, I.I., Semiletov, I.P., Tishchenko, P.Y., Pugach, S.P., and Savel'eva, N.I., 2008. Variability of the carbonate system parameters in the coast-shelf zone of the East Siberian Sea during the autumn season. *Oceanology*, **48**(1), 54-67.
- Raymond, P.A., McClelland, J.W., Holmes, R.M., Zhulidov, A.V., Mull, K., Peterson, B.J., Striegl, R.G., Aiken, G.R., and Gurtovaya, T.Y., 2007. Flux and age of dissolved organic carbon exported to the Arctic Ocean: A carbon isotopic study of the five largest arctic rivers, *Global Biogeochemical Cycles*, **21**(4), doi:10.1029/2007GB002934.
- Rachold, V., Eicken, H., Gordeev, V.V., Grigoriev, M.N., Hubberten, H.-W., Lisitzin, A.P., Shevchenko, V.P., and Schirmeister, L., 2004. Modern terrigenous organic carbon input to the Arctic Ocean. in *The Organic Carbon Cycle in the Arctic Ocean*, edited by R.S. Stein and R.W. Macdonald, pp. 33–69, Springer, New York.
- Riebesell U., Fabry V. J., Hansson L. & Gattuso J.-P. (Eds.), 2010. Guide to best practices for ocean acidification research and data reporting, 260 p. Luxembourg: Publications Office of the European Union.

- Roach A.T., Aagaard, K., Pease, C.H., Salo, S.A., Weingartner, T.J., Pavlov, V., and Kulakov, M., 1995. Direct measurements of transport and water properties through Bering Strait. *Journal of Geophysical Research*, **100**(C9), 18,443–18,457.
- Sabine, C.L. and Feely, R.A., 2007. The oceanic sink for carbon dioxide. In D. Reay, N. Hewitt, J. Grace and K. Smith, Eds. *Greenhouse Gas Sinks*. pp. 31–49. CABI Publishing, Oxfordshire, UK.
- Sabine, C.L., Feely, R.A., Gruber, N., Key, R. M., Lee, K., Bullister, J.L., Wanninkhof, R., Wong, C.S., Wallace, D.W.R., Tilbrook, B., Millero, F. J., Peng, T.-H., Kozyr, A., Ono, T., and Rios, A.F., 2004. The Oceanic Sink for Anthropogenic CO₂. *Science*, **305**(5682), 367–371.
- Semiletov, I.P., 1999. Aquatic sources of CO₂ and CH₄ in the Polar regions. *Journal of Atmospheric Sciences*, **56**(2), 286–306.
- Springer, A.M., McRoy, C.P., and Flint, M.V., 1996. The Bering Sea Green Belt: shelf-edge processes and ecosystem production. *Fisheries Oceanography*, **5**(3-4), 205–223.
- Steinacher, M., Joos, F., Frolicher, T.L., Plattner, G.-K., and Doney, S.C., 2009. Imminent ocean acidification of the Arctic projected with the NCAR global coupled carbon-cycle climate model. *Biogeosciences*, **6**, 515–533.
- Wang, W.Q., Yang, X.T., Huang, H.B., and Chen, L.Q., 2003. Investigation on distribution and fluxes of sea–air CO₂ of the expedition areas in the Arctic Ocean. *Science in China Series D—Earth Sciences*, **46**, 569–580.
- Weiss, R.F., 1974. Carbon dioxide in water and seawater: The solubility of a non-ideal gas. *Marine Chemistry*, **2**, 203–215.
- Woodgate, R.A., Aagaard, K., and Weingartner, T.J., 2005. Monthly temperature, salinity and transport variability of the Bering Strait through flow. *Geophysical Research Letters*, **32** (4), L04601, doi:10.1029/2004GL021880.
- Wright, S. W. 2005, Analysis of phytoplankton populations using pigment markers, Course notes for a workshop *Pigment Analysis Of Antarctic Microorganisms*.
- Yamamoto-Kawai M., McLaughlin F.A., Carmack, E.C., Nishino, S., and Shimada K., 2009. Aragonite undersaturation in the Arctic Ocean: effects of ocean acidification and sea ice melt. *Science*, **326**(5956), 1098–1100, doi: 10.1126/science.1174190.
- Zachos, J.C., Röhl, U., Schellenberg, S.A., Sluijs, A., Hodell, D.A., Kelly, D.C., Thomas, E., Nicolo, M., Raffi, I., Lourens, L.J., McCarren, H., Kroon, D., 2005. Rapid Acidification of the Ocean During the Paleocene-Eocene Thermal Maximum. *Science*, Vol. 308. no. 5728, pp. 1611 – 1615.